The $A = 8$ isotriplet in Fermionic Molecular Dynamics

KR Henninger

GSI Helmholtzzentrum für Schwerionenforschung GmbH, Planckstrasse 1, 64291 Darmstadt, Germany

E-mail: k.henninger@gsi.de

Abstract. Nuclear structure of the $A = 8$ isotriplet is investigated in the Fermionic Molecular Dynamics (FMD) model. All three nuclei have importance to astrophysics, and exhibit clustering or haloes. FMD uses a wave-packet basis and is well-suited for modelling such structures. For a multiconfiguration treatment we construct the many-body Hilbert space from antisymmetrised angular-momentum projected 8-particle states. First results show formation of a proton halo in ^{8}B, and reasonable reproduction of the T=1 states in ^{8}Be.

1. Introduction

Determination of stellar nucleosynthetic reaction rates may rely on input from nuclear structure calculations: experimentally, these reactions are very low-yield at astrophysical energies, giving large uncertainties and necessitating theoretical input [1]. Weakly-bound nuclei appear as intermediates in these reactions, meaning that calculation of these reaction rates often requires modeling of weakly-bound nuclear structure. Modeling such is, however, challenging, due to proximity to the continuum, which requires that one access both scattering states and compact ("shell-model like") configurations in one's chosen model, ideally in a consistent way. This is particularly relevant to the asymptotic part of the wave function (*i.e.* at distances large compared to the nuclear radius), where the scattering solutions contribute strongly ("coupling to the continuum"). Asymptotic structure may influence reaction rate heavily [2], making accurate modeling thereof an important goal.

Fermionic Molecular Dynamics (FMD) [3] is a microscopic nuclear model whose chief benefit is in accessing clustering and shell-model like states in a consistent way, due to its flexible basis (see *e.g.* [4]). The aim of this study is to model the nuclei ^{8}Li, ^{8}Be and ^{8}B in the FMD model, with a view to astrophysical applications.

Decay of ^{8}B to ^{8}Be gives rise to almost the entire high-energy solar-neutrino flux [5], making ^{8}B structure important both for determining the solar core temperature [5] and reducing uncertainty in the Standard Solar Model, where the S factor (S_{17}) for ^{7}Be(p,γ)^{8}B is imprecisely known [6, 7]. Other features in this isotriplet include the two-alpha cluster structure of the ^{8}Be ground state, which is challenging to model, especially if modeling the higher-lying, compact T=1 states consistently. ^{8}Li is of interest as the "mirror" of ^{8}B: phenomena like Thomas-Ehrman shift [8–10] are worth a revisit in mirror pairs where one nucleus has a proton halo.

2. Fermionic Molecular Dynamics

Starting with protons and neutrons as basic nuclear constituents, we choose intrinsic many-body configurations $|Q\rangle$ that are Slater determinants of single-particle states $|q\rangle$, or [11]:

$$|Q\rangle = \hat{\mathcal{A}}\left\{|q_1\rangle \otimes ... \otimes |q_A\rangle\right\} \tag{1}$$

where $\hat{\mathcal{A}}$ is the antisymmetrisation operator. The single-particle states corresponding to the protons and neutrons are:

$$|q\rangle = \sum_i |a_i, \vec{b}_i\rangle \otimes |\chi_i^{\uparrow}, \chi_i^{\downarrow}\rangle \otimes |\xi_i\rangle c_i, \tag{2}$$

where a superposition of wave-packets $|a_i, \vec{b}_i\rangle$ in the spatial part aids description of extended distributions (*e.g.* haloes). Parameters $\vec{b}$ relate to the mean position and mean momentum of the wave-packets and parameters a to their width [12]. The ket $|\chi^{\uparrow}, \chi^{\downarrow}\rangle$ is the most general spinor. The isospin part $|\xi\rangle$ defines a particle as a proton or neutron, allowing no superpositions of the two.

In phase space, the nucleon wave functions are Gaussian wavepackets, *e.g.* in co-ordinate space we have:

$$\langle \vec{x}|q\rangle = \exp\left\{-\frac{(\vec{x}-\vec{b})^2}{2a}\right\}. \tag{3}$$

It is necessary to project out of intrinsic states $|Q\rangle$ the eigenstates of angular momentum and parity, via projection operators [12]:

$$\hat{P}^{\pi} = \frac{1}{2}(1 + \pi\hat{\Pi})$$
$$\hat{P}^{J}_{MK} = \frac{2J+1}{8\pi^2}\int d\Omega\, D^{J}_{MK}(\Omega)^{*}\hat{R}(\Omega),$$

where $D^{J}_{MK}(\alpha,\beta,\gamma)$ is the Wigner D-matrix, $\hat{R}(\alpha,\beta,\gamma)$ and $\hat{\Pi}$ are rotation and parity operators and $\Omega = \{\alpha,\beta,\gamma\}$ symbolises the Euler angles.

To obtain a good approximation to the nuclear ground state, the parameters $\{q_\nu\}$ describing the intrinsic basis states $|Q\rangle$ are evaluated by requiring [4]:

$$\min_{\{q_\nu\}} \quad \frac{\langle Q|\hat{H} - \hat{T}_{cm}|Q\rangle}{\langle Q|Q\rangle}, \tag{4}$$

where including the operator $\hat{T}_{cm}$ ensures that centre-of-mass kinetic energy is subtracted out. Using Eq.(4) is called Projection after Variation (PAV), as the variational principle is applied and then projection operators act on the minimised state. It is more accurate to vary energy of the projected state (Variation After Propection (VAP)), as then it is certain the projected state has minimum energy [4].

To improve the description, additional basis states can be generated by performing minimisation (Eq.(4)) subject to various constraints. These constraints could be on *e.g.* radii, moments or deformation parameters [4]; allowing inclusion of many different configurations in the basis thus created. The Hamiltonian may then be diagonalised in this basis. One may also create basis states in which one explicitly imposes that the nucleus is composed of 2 or 3 clusters [4], which may then be added to the constrained VAP basis to improve the description of the asymptotic region.

2.1. Interactions for FMD

FMD requires the Hamiltonian to be in operator form, so short range correlations are treated via the Unitary Correlation Operator Method (UCOM) (see refs [13–15]).

The UCOM involves applying a unitary correlation operator $\hat{C}$ to the many-body state, to incorporate the short-range correlations. This gives rise to an effective Hamiltonian $\hat{H}_{eff}$, as [14]:

$$\begin{aligned}\langle\Psi|\hat{C}^\dagger\hat{H}\hat{C}|\Psi\rangle &= \langle\tilde{\Psi}|\hat{H}|\tilde{\Psi}\rangle \\ &= \langle\Psi|\hat{H}_{eff}|\Psi\rangle,\end{aligned}$$

where $\hat{H}_{eff} = \hat{C}^\dagger\hat{H}\hat{C}$ and $\hat{C}|\Psi\rangle = |\tilde{\Psi}\rangle$.

This transformation of the Hamiltonian induces many-body terms, *i.e.* [14]:

$$\hat{H}_{eff} = \hat{H}^{[1]}_{eff} + \hat{H}^{[2]}_{eff} + \hat{H}^{[3]}_{eff} + \cdots, \tag{5}$$

where the number in square brackets indicates number of bodies involved. The estimated contribution of the three- and higher-body terms turns out to be very small compared to the two-body contribution [13]. The transformed Hamiltonian up to two-body is therefore what one calls the UCOM Hamiltonian. One compensates for "missing" three-body and higher terms by adjusting the strength factor of the spin-orbit term, according to what best reproduces the nuclear observables. In these calculations, we use a UCOM-transformed Argonne $v18$ (AV18) interaction [16], as No-Core Shell Model calculations using this interaction show it to give good descriptions of light p-shell nuclei [14].

3. Calculations

A VAP basis set was created for each of the three nuclei (^{8}Li, ^{8}Be and ^{8}B), using constraints on matter radius. Using the same constraint for all three nuclei ensures that one may compare results. The maximum basis size was chosen by adding states to the basis, diagonalising, and looking for convergence behaviour in energies of the low-lying states (see Fig. 1).

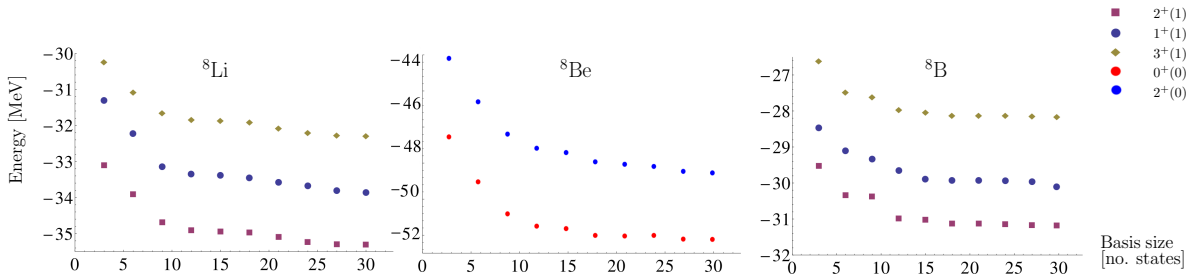

Figure 1: Energies of the low-lying states of the $A = 8$ nuclei, plotted with basis size, indicating convergence behaviour as basis size is increased. States are labelled with spin, parity and isospin as in the key.

In order to compare results for the whole isomultiplet, it was decided to add the isospin partner states into each basis. These are obtained for the ^{8}Li-^{8}B mirror pair via rotations in isospin space, or

$$|\tilde{Q}\rangle = exp\left\{i\pi\hat{T}_2\right\}|Q\rangle = exp\left\{i\pi\sum_j \hat{t}_2(j)\right\}\left(\mathcal{A}\left\{|t(1),t_3(1)\rangle\otimes\ldots\otimes|t(A),t_3(A)\rangle\right\}\right), \tag{6}$$

where $|t(j), t_3(j)\rangle$ represents the isospin state of the jth nucleon, $|\tilde{Q}\rangle$ is a state in ^{8}B and $|Q\rangle$ is a state in ^{8}Li, say. For transforming states in ^{8}Li or ^{8}B to states in ^{8}Be, formally one applies the isospin raising and lowering operators. In practise, one successively changes each of the five protons to a neutron in each radius-constrained ^{8}B basis state $|Q\rangle$ (or *vice versa*); giving 5 new ^{8}Be basis states for each $|Q\rangle$ of ^{8}B or ^{8}Li. The two methods are equivalent: With isospin raising and lowering operators, one would obtain a linear combination of these aforementioned states, but we will reach such a linear combination when diagonalizing the Hamiltonian in this basis.

Besides creation and selection of basis states, one also has to consider the strength factor of the spin-orbit term, as this incorporates the three- and higher-body terms in the interaction. We initially perform all calculations using a spin-orbit strength factor of 2, and then used calculated transition-strengths and energies as an indicator for adjusting the strength. In the case of weakly-bound nuclei with spatially-extended structures, (such as ^{8}B), one may need less spin-orbit strength. In ^{8}Be, the T=1 states are more compact than the (α-cluster based) T=0 states, and will thus be affected more strongly by three- and higher-body forces. We thus try larger values of the spin-orbit strength factor when treating ^{8}Be. Results and selected strength factors are discussed below (Section 4).

4. Results

4.1. Observables

For all three nuclei, one obtains energy-levels that compare quite favourably to experiment (Fig. 2), and especially to the calculated thresholds, in all three cases. The final basis set used for each nucleus is summarised in Table 3. The calculated thresholds are ground-state energies of the relevant core nuclei, calculated in radius-constrained FMD basis sets of comparable dimension to those for the nuclei of interest. In the case of ^{8}Li, the ^{7}Li+n threshold was calculated (making ^{7}Li the core nucleus), for ^{8}Be, the two α particle threshold, and for ^{8}B the ^{7}Be+p threshold.

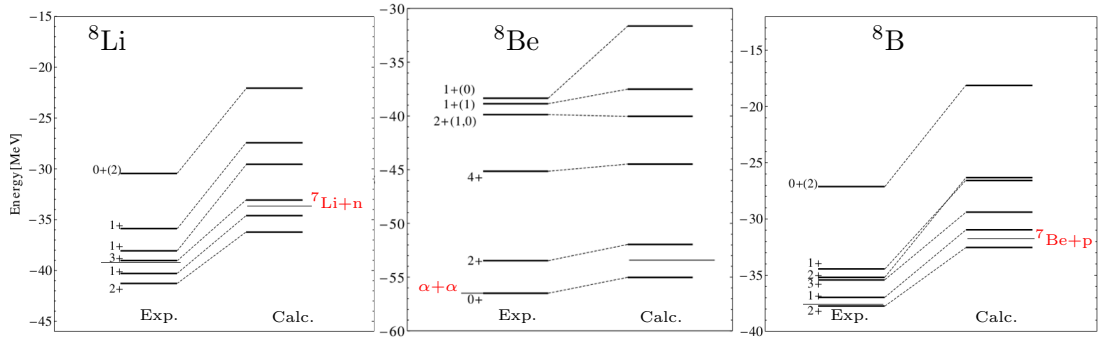

Figure 2: Experimental and calculated level-schemes for nuclei of the A=8 isotriplet. Basis sets used are described in Table 3. Note the different y-axes for energy. The thin horizontal lines indicate experimental and calculated thresholds for the decay process indicated (red labels).

Table 1: Transition strengths for some intense transitions in the A=8 nuclei. Measured values from [17–19]. "Exp." and "Calc." indicate experimental and calculated energies. Numbers in round braces indicate the strength of the spin-orbit term. Transition strengths were calculated in the "full" basis (supplied in Table 3).

	States	Energies [MeV]				Transition strengths			
		Exp.	Calc. (1.5)	Calc. (2.0)	Calc. (3.0)	Exp.	Calc.(1.5)	Calc. (2.0)	Calc. (3.0)
^{8}Li	$1^+ \rightarrow 2^+$	0.980	1.261	1.622	2.541	5.00(16) μ_N^2	5.080 μ_N^2	5.317 μ_N^2	5.825 μ_N^2
^{8}Be	$2^+ \rightarrow 0^+$	3.03	3.387	3.367	3.117	25(8) e^2fm^4	21.175 e^2fm^4	18.515 e^2fm^4	12.281 e^2fm^4
^{8}B	$1^+ \rightarrow 2^+$	0.77	1.207	1.570	2.521	4.71(21) μ_N^2	4.267 μ_N^2	4.385 μ_N^2	4.915 μ_N^2

Table 2: Calculated rms radii for ground states of the A=8 isotriplet. References for the experimental values are in square brackets. Radii were calculated in the "full" basis (as in Table 3). Numbers in round braces indicate the strength of the spin-orbit term.

		R_{matter} [fm]	R_p [fm]	R_n [fm]	R_{charge} [fm]
^{8}Li	Exp.	2.37(2) [20]	-	-	2.29(8) fm [21]
	Calc. (1.5)	2.315	2.118	2.430	2.255
	Calc. (2.0)	2.243	2.070	2.341	2.211
^{8}Be	Calc.(2.0)	2.404	2.408	2.400	2.545
	Calc.(3.0)	2.278	2.282	2.274	2.427
^{8}B	Exp.	2.38(4) [20]	-	-	-
	Calc.(1.5)	2.367	2.492	2.142	2.634
	Calc.(2.0)	2.282	2.389	2.091	2.537

Table 3: Details of basis sets.

Nucleus:	Basis states:
^{8}Li	45 basis states: 27 radius-constrained VAP states for ^{8}Li (9 each for $J^\pi = 1^+, 2^+, 3^+$), 11 cluster states (^{7}Li+n) and 18 isospin-partner states from ^{8}B (radius-constrained VAP states projected on $J^\pi = 1^+, 2^+, 3^+$).
^{8}Be	260 basis states: 24 radius-constrained VAP states for ^{8}Li (8 each for $J^\pi = 0^+, 2^+, 4^+$), 11 cluster states (2-α) and 225 isospin-partner states from ^{8}B and ^{8}Li (radius-constrained VAP states projected = J^π of $1^+, 2^+, 3^+$).
^{8}B	45 basis states: 18 radius-constrained VAP states for ^{8}B (6 each for $J^\pi = 1^+, 2^+, 3^+$), 11 cluster states (^{7}Be+p) and 27 isospin-partner states from ^{8}Li (radius-constrained VAP states projected on $J^\pi = 1^+, 2^+, 3^+$).

4.2. Spin-orbit strength factor

As discussed, we choose a spin-orbit strength factor that best incorporates higher-body terms. We deduce from reproduction of observables (Tables 1-2) that spin-orbit strength factor 1.5 is preferable for ^{8}Li, and factor 2 for ^{8}B (radii are better-reproduced with factor 1.5, but transitions and energies with factor 2). Spin-orbit strength strongly affects energy of ^{8}Be T=1 states (Fig. 3). The T=1 states are well-reproduced when using a spin-orbit strength factor 3.

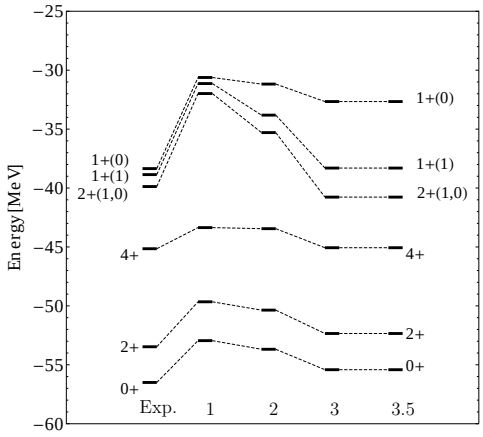

Figure 3: Level-schemes for ^{8}Be, comparing experimental and calculated energies when strength factor of the spin-orbit term is varied. Numbers below each band indicate the strength factor of the spin-orbit term.

4.3. Comparison to No-Core Shell Model

Our results are compared to current many-body theoretical results from the No-Core Shell Model (NCSM) in Fig. 4. The NCSM calculations of [19] use an interaction obtained from chiral effective field theory (χ-EFT). We compare to the energies they obtain using a χ-EFTH interaction with up to two body terms included because the UCOM-transformed AV18 is truncated at two-body, as discussed. In order to compare to their calculations using two-body forces, we performed calculations using the UCOM-transformed AV18 with an $L \cdot S$ term with strength factor 1. Our calculations compare relatively well with theirs, especially as regards binding relative to threshold. The model-space of [19] is an $8\hbar\Omega$ space.

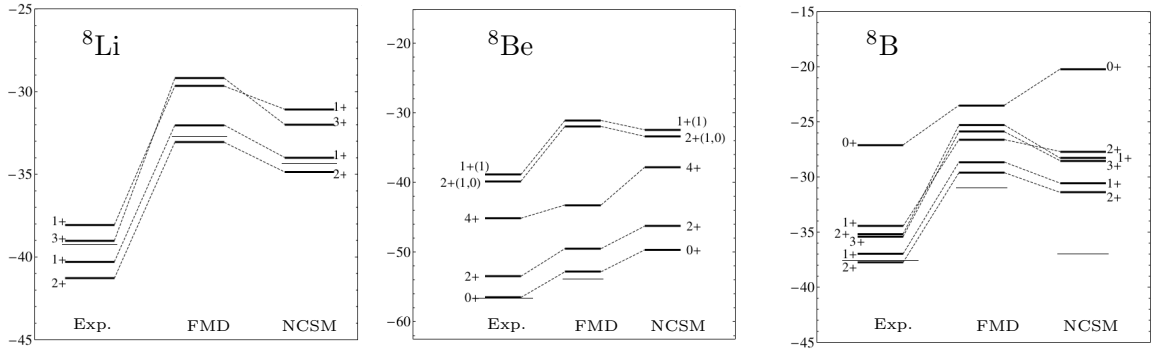

Figure 4: Our results for the A=8 isotriplet (FMD), compared to NCSM results of [19] (NCSM). Both are compared to the experimental levels (Exp). The FMD results shown here were calculated using a spin-orbit term with strength factor 1, as the NCSM energy-levels shown were calculated using a χ-EFT interaction truncated at the two-body level. Note the different y-axes for energy. The thin horizontal lines indicate experimental and calculated thresholds, which are the same as those in Fig. 2. The NCSM results were calculated in an $8\hbar\omega$ model-space.

5. Conclusion and Summary

The results obtained here show that our FMD calculations reproduce energies, transition-strengths and radii of the A=8 isotriplet nuclei favourably, and compare well with the latest theoretical results. Our results show formation of a proton halo in ^{8}B (a calculated proton radius of 2.389 fm, neutron radius of 2.091 fm and matter radius of 2.282 fm).We also achieve reasonable reproduction of the T=1 states in ^{8}Be; which indicates FMD is able to reproduce both clustering and shell-model like states consistently.

Acknowlegements

The author thanks Prof. Dr Hans Feldmeier and Dr Thomas Neff for extensive and expert guidance throughout the work.

References

[1] C.E. Rolfs and W.S. Rodney. *Cauldrons in the Cosmos: Nuclear Astrophysics.* The University of Chicago Press, Chicago, 1988. Pp 150, 156, 493.
[2] K. Riisager and A.S. Jensen. *The radius of ^{8}B and Solar Neutrinos.* Phys. Lett. ***B***, **301**:6, 1993.
[3] H. Feldmeier. *Fermionic Molecular Dynamics.* Nucl. Phys., **A515**:147, 1990.
[4] T. Neff and H. Feldmeier. Cluster Structure in the Fermionic Molecular Dynamics approach. In M. Brenner, editor, *Cluster Structure of Atomic Nuclei*, pages 67–94. Research Signpost publishing, 2010.
[5] R. E. Tribble A. M. Mukhamedzhanov H.M. Xu, C. A. Gagliardi and N. K. Timofeyuk. *Overall Normalization of the Astrophysical S-factor and the Nuclear Vertex Constant for ^{7}Be(p,γ)^{8}B Reactions.* Phys. Rev. Lett, 73:2027, 1994.
[6] A. Csòtò. *Off-Shell Effects in the Energy-Dependence of the ^{7}Be(p,γ)^{8}B Astrophysical S-factor.* Phys. Lett. ***B***, **394**:247, 1997.
[7] P.D. Parker W.C. Haxton and C.E. Rolfs. *Solar Hydrogen burning and neutrinos.* Nucl. Phys., **A777**:226, 2006.
[8] R.G. Thomas. *An Analysis of the Energy Levels of the Mirror Nuclei, ^{13}C and ^{13}N.* Phys. Rev., **88**:1109, 1952.
[9] J. B. Ehrman. *On The Displacement of Corresponding Energy Levels of ^{13}C and ^{13}N.* Phys. Rev., **81**:412, 1951.
[10] JA Nolen and JP Schiffer. *Coulomb Energies.* Ann. Rev. Nucl. Sci., **19**:472, 1969.
[11] H. Feldmeier and J. Schnack. *Fermionic Molecular Dynamics.* Prog. Part. Nucl. Phys., **39**:343, 1997.
[12] T. Neff and H. Feldmeier. *Clustering and Other Exotic Phenomena in Nuclei.* Eur. Phys. J., **156**:69, 2008.
[13] T. Neff H. Feldmeier, R. Roth and J. Schnack. *A Unitary Correlation Operator Method.* Nucl. Phys., **A632**:61, 1998.
[14] T. Neff R. Roth and H. Feldmeier. *Nuclear Structure in the Framework of the Unitary Correlation Operator Method.* Prog. Part. Nucl. Phys., **65**:50, 2010.
[15] T. Neff and H. Feldmeier. *Tensor Correlations in the Unitary Correlation Operator Method.* Nucl. Phys. ***A***, **713**:311, 2003.
[16] R. Schiavilla R. B. Wiringa, B.G.J. Stokes. *Accurate Nucleon-Nucleon Potential with Charge-Independence Breaking.* Phys. Rev ***C***, **51**:38, 1995.
[17] J.L.Godwin D.J. Millener J.E. Purcell C.G.Sheu D.R. Tilley, H.Kelley and H.R.Weller. *Energy Levels of Light Nuclei A = 8,9,10.* Nucl. Phys. , **A745**:155, 2004 (revised 2014).
[18] D.R. Chakrabarty V. Nanal E.T. Mirgule A. Mitra V.M. Datar, S. Kumar and H.H. Oza. *Direct Observation of the 4+-to-2$^+$ Gamma Transition in ^{8}Be.* Phys. Rev. Lett., **94**:122502, 2005.
[19] J.P. Vary P. Maris and P. Navratil. *Structure of A=7-8 nuclei with two- plus three-nucleon interactions from Chiral EFT.* Phys. Rev. C, **87**:014327, 2013.
[20] T. Suzuki A. Ozawa and I. Tanihata. *Nuclear Size and Related Topics* . Nucl. Phys. **A**, **693**:32, 2001.
[21] A. Dax S. Götte R. Kirchner H.-J. Kluge Th. Kühl R. Sanchez A. Wojtaszek B. A. Bushaw G. W. F. Drake Z.-C. Yan G. Ewald, W. Nörtershäuser and C. Zimmermann. *Nuclear Charge Radii of ^{8,9}Li determined by Laser Spectroscopy.* Phys. Rev. Lett., **93**:113002, 2004.